IEEE Access
Multidisciplinary | Rapid Review | Open Access Journal

SPECIAL SECTION ON NEW WAVEFORM DESIGN AND AIR-INTERFACE FOR FUTURE HETEROGENEOUS NETWORK TOWARDS 5G

Received February 19, 2019, accepted March 5, 2019, date of publication March 8, 2019, date of current version March 29, 2019.

Digital Object Identifier 10.1109/ACCESS.2019.2903909

Orthogonally Polarized Dual-Channel Directional Modulation Based on Crossed-Dipole Arrays

BO ZHANG[1], (Member, IEEE), WEI LIU[2], (Senior Member, IEEE), AND XIANG LAN[2]

[1]College of Electronic and Communication Engineering, Tianjin Normal University, Tianjin 300387, China
[2]Communications Research Group, Department of Electronic and Electrical Engineering, The University of Sheffield, Sheffield S1 4ET, U.K.

Corresponding authors: Bo Zhang (b.zhangintj@outlook.com) and Wei Liu (w.liu@sheffield.ac.uk)

ABSTRACT Directional modulation (DM) as a physical layer security technique has been studied based on the traditional antenna arrays; however, in most of the designs, only one signal is transmitted at one carrier frequency. In this paper, signal polarization information is exploited, and a new DM scheme is designed, which can transmit a pair of orthogonally polarized signals to the same direction at the same frequency simultaneously, resulting in doubled channel capacity. These two signals can also be considered as one composite signal using a four-dimensional (4-D) modulation scheme across the two polarization diversity channels. Moreover, compressive sensing (CS)-based formulations for designing sparse crossed-dipole arrays in this context are proposed to exploit the degrees of freedom in the spatial domain for further improved performance, as demonstrated by various design examples.

INDEX TERMS Crossed-dipole array, directional modulation, orthogonal polarization.

I. INTRODUCTION

Directional modulation (DM) as a physical layer security technique was introduced in [1] and [2] by keeping desired constellation points in an interested direction or directions, while scrambling them for the remaining directions. A procedure based on reconfigurable antenna arrays on how to switch elements for transmitting symbols un-distorted in a specified direction was described in [3]. Phased arrays were also applied to the DM design with a single carrier frequency [4], [5] and multi-carrier frequencies [6]. Multiple input multiple output (MIMO) and artificial-noise (AN)-aided designs [7]–[10] were used to achieve DM as well. In [11], a dual-beam DM scheme was proposed to synthesize a DM signal, where unlike the traditional transmitter, the in-phase and quadrature signals were excited by two antennas. In [12], a DM based two element antenna array was studied, followed by a pattern synthesis method in [13], an artificial-noise-aided zero-forcing synthesis approach in [14], and a multi-relay design in [15]. Static and dynamic interference were combined together and added into the DM design, then a more security performance based on the same level of transmission power can be achieved [16]. Recently, DM was extended to multi-path channel models [17], [18], which helps improve security of the system when the eavesdroppers are very close to the desired position, and DM was also applied to sparse array design [18] to further exploit the degrees of freedom (DOFs) in the spatial domain.

However, in the current DM field, only one signal is transmitted at one carrier frequency to the desired direction. To increase channel capacity, in this paper we exploit the polarization information of the electromagnetic signal, and two orthogonally polarized signals can be transmitted to the same direction at the same frequency simultaneously without crossover, as demonstrated in our recent conference publication [19]. These two signals can also be considered as one composite signal using the four dimensional (4-D) modulation scheme across the two polarisation diversity channels [20]–[22]. This can be achieved by employing polarisation-sensitive arrays, such as tripole arrays and crossed-dipole arrays [20], [23]–[30]. To receive and separate the two orthogonally polarized signals, a crossed-dipole antenna or array can be employed at the receiver side [30], and polarizations of the antennas at the receiver side do not need to match those of the transmitters, as cross-interference due to a mismatch or channel distortion can be suppressed using standard signal processing techniques, such as the Wiener filter when a reference signal is available [20].

Moreover, compared to [19], to reduce the number of antennas and further exploit the DOFs [31], [32] in the

The associate editor coordinating the review of this manuscript and approving it for publication was Qilian Liang.

spatial domain, the orthogonally polarized design for DM is applied to sparse antenna arrays. In this work, similar to the design in [5] and [6], we apply compressive sensing (CS) based formulation to the design. In the context of M-ary signaling for modulation, assume there are M symbols for each of the two signals s_1 and s_2. Then, for the two signals transmitted simultaneously, there will be M^2 combined symbols in total. The key is to find a set of common crossed-dipole locations for all M^2 combined symbols, which can be solved using the group sparsity technique [33]; otherwise, we would have different antenna locations for different combined symbols.

Overall, the contribution of the work is two-fold: firstly, we exploit the polarisation information and extend the traditional DM design to the dual-polarized antenna arrays; secondly, a sparse array design method is proposed to reduce the number of dual-polarized antennas by exploiting the DOFs in the spatial domain.

The remaining part is organized as follows. A review of crossed-dipole arrays is given in Sec. II. DM design for a pair of orthogonally polarized signals transmitted from a given array geometry and an array with optimized crossed-dipole locations are considered in Sec. III. Design examples are presented in Sec. IV and conclusions drawn in Sec. V.

II. POLARIZATION-SENSITIVE BEAMFORMING BASED ON CROSSED-DIPOLE ARRAYS

Fig. 1 shows the structure of an N-element linear crossed-dipole array. Each antenna has two orthogonally orientated dipoles, one parallel to the x-axis with a complex-valued coefficient $w_{n,x}$, and one parallel to the y-axis with coefficient $w_{n,y}$, $n = 0, \ldots, N-1$. The zeroth antenna located at the transmitter coordinate origin is assumed as the reference point. The spacing between the zeroth and the n-th antenna is denoted by d_n ($n = 1, \ldots, N-1$), and the aperture of the array is d_{N-1}. The elevation angle and azimuth angle are denoted by $\theta \in [0, \pi]$ and $\phi \in [0, 2\pi]$, respectively.

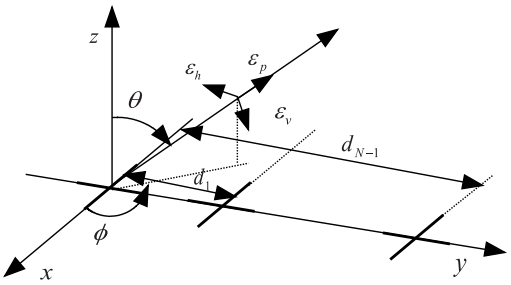

FIGURE 1. A linear crossed-dipole array.

For a transverse electromagnetic (TEM) wave in the far-field from the transmitter array, ε_p is considered as the unit vector of the transmission direction of the TEM wave, and ε_h and ε_v are two orthogonal unit vectors and also at right angle to ε_p, i.e., $\varepsilon_h \cdot \varepsilon_v = 0$, $\varepsilon_h \cdot \varepsilon_p = 0$, and $\varepsilon_v \cdot \varepsilon_p = 0$. Based on the transmission direction in the transmitter coordinate system, we have

$$\varepsilon_p = [\sin\theta\cos\phi, \sin\theta\sin\phi, \cos\theta]^T, \tag{1}$$

where $\{\cdot\}^T$ is the transpose operation. The choice of ε_h and ε_v is not unique. Based on the orthogonality of these three unit vectors, normally we assume

$$\begin{aligned}\varepsilon_h &= [-\sin\phi, \cos\phi, 0]^T,\\ \varepsilon_v &= [\cos\theta\cos\phi, \cos\theta\sin\phi, -\sin\theta]^T.\end{aligned} \tag{2}$$

Here it can be seen that ε_h is parallel to the x-y plane, due to the zero value in the z direction, then ε_h is assumed as the unit vector of the horizontal component. Since ε_v is perpendicular to ε_p ($\varepsilon_v \cdot \varepsilon_p = 0$), ε_v is considered as the unit vector of the vertical component.

Moreover, we assume the electric field has transverse components [23], [24],

$$E = E_h\varepsilon_h + E_v\varepsilon_v, \tag{3}$$

where E_h and E_v correspond to the horizontal component and the vertical component, respectively [34], given by

$$\begin{bmatrix} E_h \\ E_v \end{bmatrix} = \begin{bmatrix} He^{j\omega t} \\ Ve^{j\omega t} \end{bmatrix} = \begin{bmatrix} a_h e^{j\psi_h} e^{j\omega t} \\ a_v e^{j\psi_v} e^{j\omega t} \end{bmatrix}, \tag{4}$$

where ω represents carrier frequency, H and V are complex numbers, a_h and a_v are amplitudes (positive and real-valued) of the horizontal and vertical components, and ψ_h and ψ_v are the corresponding initial phases. The polarisation ratio is represented by $\frac{V}{H} = \frac{a_v e^{j\psi_v}}{a_h e^{j\psi_h}} = (\tan\gamma)e^{j\eta}$ for $\gamma \in [0, \pi/2]$ and $\eta \in (-\pi, \pi]$, where $\tan\gamma$ represents the amplitude ratio, and η is the phase difference between two components [34]. Then the electric field can be given by

$$\begin{aligned} E &= E_h\varepsilon_h + E_v\varepsilon_v \\ &= A((\cos\gamma)\varepsilon_h + (\sin\gamma)e^{j\eta}\varepsilon_v) \\ &= A((-\cos\gamma\sin\phi + (\sin\gamma)e^{j\eta}\cos\theta\cos\phi)\hat{x} \\ &\quad + (\cos\gamma\cos\phi + (\sin\gamma)e^{j\eta}\cos\theta\sin\phi)\hat{y} \\ &\quad - ((\sin\gamma)e^{j\eta}\sin\theta)\hat{z}), \end{aligned} \tag{5}$$

where the amplitude A of the polarized signal is $A = \sqrt{|H|^2 + |V|^2}$, and the carrier wave $e^{j\omega t}$ is ignored. Considering the x- and y-axes where these dipoles are placed, the spatial-polarisation coherent vector $\mathbf{s}_p$ [30], [35] can be given by

$$\begin{aligned} \mathbf{s}_p(\theta, \phi, \gamma, \eta) &= \begin{bmatrix} s_{px}(\theta, \phi, \gamma, \eta) \\ s_{py}(\theta, \phi, \gamma, \eta) \end{bmatrix} \\ &= \begin{bmatrix} -\cos\gamma\sin\phi + (\sin\gamma)e^{j\eta}\cos\theta\cos\phi \\ \cos\gamma\cos\phi + (\sin\gamma)e^{j\eta}\cos\theta\sin\phi \end{bmatrix}. \end{aligned} \tag{6}$$

The spatial steering vector of the array for transmission is a function of θ and ϕ, given by

$$\mathbf{s}_s(\theta, \phi) = [1, e^{-j\omega d_1 \sin\theta\sin\phi/c}, \ldots, e^{-j\omega d_{N-1}\sin\theta\sin\phi/c}]^T, \tag{7}$$

where c is the speed of propagation. The steering vector of the array is the Kronecker product of spatial-polarisation coherent vector $\mathbf{s}_p(\theta, \phi, \gamma, \eta)$ and spatial steering vector $\mathbf{s}_s(\theta, \phi)$. Then, the steering vectors of the two sub-arrays can be given by

$$\begin{aligned}\mathbf{s}_x(\theta, \phi, \gamma, \eta) &= s_{px}(\theta, \phi, \gamma, \eta)\mathbf{s}_s(\theta, \phi),\\ \mathbf{s}_y(\theta, \phi, \gamma, \eta) &= s_{py}(\theta, \phi, \gamma, \eta)\mathbf{s}_s(\theta, \phi).\end{aligned} \tag{8}$$

The beam response of the array is [36]

$$p(\theta, \phi, \gamma, \eta) = \mathbf{w}^H \mathbf{s}(\theta, \phi, \gamma, \eta), \tag{9}$$

where $\{\cdot\}^H$ represents the Hermitian transpose, $\mathbf{s}(\theta, \phi, \gamma, \eta)$ is the $2N \times 1$ steering vector of the array

$$\begin{aligned}\mathbf{s}(\theta, \phi, \gamma, \eta) &= [\mathbf{s}_x(\theta, \phi, \gamma, \eta), \mathbf{s}_y(\theta, \phi, \gamma, \eta)]^T,\\ \mathbf{s}_x(\theta, \phi, \gamma, \eta) &= [s_{0,x}(\theta, \phi, \gamma, \eta), \ldots, s_{N-1,x}(\theta, \phi, \gamma, \eta)]^T,\\ \mathbf{s}_y(\theta, \phi, \gamma, \eta) &= [s_{0,y}(\theta, \phi, \gamma, \eta), \ldots, s_{N-1,y}(\theta, \phi, \gamma, \eta)]^T,\end{aligned} \tag{10}$$

and $\mathbf{w}$ is the complex-valued weight vector

$$\mathbf{w} = [w_{0,x}, \ldots, w_{N-1,x}, w_{0,y}, \ldots, w_{N-1,y}]^T. \tag{11}$$

III. DIRECTIONAL MODULATION DESIGN

A. DESIGN WITH A FIXED CROSSED-DIPOLE ARRAY

In the current DM field, there is only one signal transmitted at one carrier frequency to the desired direction, and the weight coefficients are thus designed for one single signal. To increase channel capacity, in this section, we design a new DM scheme where a pair of orthogonally polarized signals can be transmitted at the same carrier frequency simultaneously without crossover. In detail, we need to find a set of weight coefficients for these two signals (s_1 and s_2). We use $\mathbf{s}(\theta, \phi, \gamma_1, \eta_1)$, $\mathbf{s}(\theta, \phi, \gamma_2, \eta_2)$, $p(\theta, \phi, \gamma_1, \eta_1)$, and $p(\theta, \phi, \gamma_2, \eta_2)$ to represent the steering vectors for s_1 and s_2, and beam responses for s_1 and s_2, respectively.

Here, we assume ϕ is fixed, and r points in the mainlobe and $R-r$ points in the sidelobe for both s_1 and s_2 are sampled. Then, we can construct a $2N \times 2r$ matrix $\mathbf{S}_{ML}$ for steering vectors of two signals in the mainlobe, and a $2N \times 2(R-r)$ matrix $\mathbf{S}_{SL}$ including all steering vectors over the sidelobe range [6],

$$\begin{aligned}\mathbf{S}_{SL} &= [\mathbf{s}(\theta_0, \phi, \gamma_1, \eta_1), \ldots, \mathbf{s}(\theta_{R-r-1}, \phi, \gamma_1, \eta_1)\\ &\quad \mathbf{s}(\theta_0, \phi, \gamma_2, \eta_2), \ldots, \mathbf{s}(\theta_{R-r-1}, \phi, \gamma_2, \eta_2)],\\ \mathbf{S}_{ML} &= [\mathbf{s}(\theta_{R-r}, \phi, \gamma_1, \eta_1), \ldots, \mathbf{s}(\theta_{R-1}, \phi, \gamma_1, \eta_1)\\ &\quad \mathbf{s}(\theta_{R-r}, \phi, \gamma_2, \eta_2), \ldots, \mathbf{s}(\theta_{R-1}, \phi, \gamma_2, \eta_2)].\end{aligned} \tag{12}$$

Moreover, for M-ary signaling of modulation, each of s_1 and s_2 can create M constellation points (M symbols), leading to M desired responses. Since both signals are transmitted simultaneously, there are in total M^2 different symbols and M^2 sets of response pairs. According to the direction of the elevation angle θ, we define $\mathbf{p}_{SL,m}$ and $\mathbf{p}_{ML,m}$ as beam responses over the sidelobe and mainlobe directions for the m-th combined symbol, where $m = 0, \ldots, M^2 - 1$,

$$\begin{aligned}\mathbf{p}_{SL,m} &= [p_m(\theta_0, \phi, \gamma_1, \eta_1), \ldots, p_m(\theta_{R-r-1}, \phi, \gamma_1, \eta_1)\\ &\quad p_m(\theta_0, \phi, \gamma_2, \eta_2), \ldots, p_m(\theta_{R-r-1}, \phi, \gamma_2, \eta_2)],\\ \mathbf{p}_{ML,m} &= [p_m(\theta_{R-r}, \phi, \gamma_1, \eta_1), \ldots, p_m(\theta_{R-1}, \phi, \gamma_1, \eta_1)\\ &\quad p_m(\theta_{R-r}, \phi, \gamma_2, \eta_2), \ldots, p_m(\theta_{R-1}, \phi, \gamma_2, \eta_2)].\end{aligned} \tag{13}$$

Then, the weight coefficients for the m-th combined symbol can be solved by

$$\begin{aligned}&\min_{\mathbf{w}_m} ||\mathbf{p}_{SL,m} - \mathbf{w}_m^H \mathbf{S}_{SL}||_2\\ &\text{subject to } \mathbf{w}_m^H \mathbf{S}_{ML} = \mathbf{p}_{ML,m},\end{aligned} \tag{14}$$

where $\mathbf{w}_m = [w_{0,x,m}, \ldots, w_{N-1,x,m}, w_{0,y,m}, \ldots, w_{N-1,y,m}]^T$ corresponds to the m-th response pair $\mathbf{p}_m(\theta, \phi, \gamma, \eta) = [\mathbf{p}_{SL,m}, \mathbf{p}_{ML,m}]$, and $||\cdot||_2$ denotes the l_2 norm. The problem in (14) can be solved by the method of Lagrange multipliers and the optimum value for the coefficients $\mathbf{w}_m$ can be found in our earlier conference publication [19], which is given by

$$\begin{aligned}\mathbf{w}_m = \mathbf{R}^{-1}(\mathbf{S}_{SL}\mathbf{p}_{SL,m}^H - \mathbf{S}_{ML}((\mathbf{S}_{ML}^H \mathbf{R}^{-1} \mathbf{S}_{ML})^{-1}\\ \times (\mathbf{S}_{ML}^H \mathbf{R}^{-1} \mathbf{S}_{SL} \mathbf{p}_{SL,m}^H - \mathbf{p}_{ML,m}^H))),\end{aligned} \tag{15}$$

with $\mathbf{R} = \mathbf{S}_{SL}\mathbf{S}_{SL}^H$.

B. SPARSE ARRAY DESIGN

Uniform linear arrays (ULAs) are widely used for DM; however, this is not the most effective way to achieve DM in terms of the number of antennas. To reduce the number of antennas but keep the antenna array performance, sparse arrays can be used in the context of DM [5], [6]. The idea of sparse array design using CS-based methods is to find the minimum number of non-zero valued weight coefficients from a large number of potential antennas to generate a response close to the desired one. As antennas with zero-valued coefficients are removed, the objective function for finding the minimum number of weight coefficients can be given by $\min ||\mathbf{w}||_1$, where the l_1 norm $||\cdot||_1$ is used as an approximation to the l_0 norm $||\cdot||_0$. The constraint for keeping the difference between desired and designed responses under a given threshold value can be written as $||\mathbf{p} - \mathbf{w}^H\mathbf{S}||_2 \leq \alpha$, where α represents the allowed difference. Based on this idea of sparse array design, weight vector $\mathbf{w}_m$ for the m-th set of constellation points in (14) can be adjusted to

$$\begin{aligned}&\min_{\mathbf{w}_m} ||\mathbf{w}_m||_1\\ &\text{subject to } ||\mathbf{p}_{SL,m} - \mathbf{w}_m^H \mathbf{S}_{SL}||_2 \leq \alpha\\ &\qquad \mathbf{w}_m^H \mathbf{S}_{ML} = \mathbf{p}_{ML,m}.\end{aligned} \tag{16}$$

As the location optimization in (16) is calculated individually for each set of constellation points, a common set of active crossed-dipole positions cannot be guaranteed for all symbol pairs; in other words, the antenna with weight coefficients which are zero-valued for some symbols but non-zero-valued for others, cannot be removed. To solve the

problem, group sparsity is introduced [33] to find a common set of active antenna locations for all sets of constellation points. Therefore, we introduce $\tilde{\mathbf{w}}_n$ to allow all elements in the vector to be minimized simultaneously, e.g. to remove the n-th antenna, the vector $\tilde{\mathbf{w}}_n$ needs to be zero-valued

$$\tilde{\mathbf{w}}_n = [w_{n,x,0}, \ldots, w_{n,x,M^2-1}, w_{n,y,0}, \ldots, w_{n,y,M^2-1}]. \quad (17)$$

Then, the cost function for finding the minimum number of antenna locations can be considered as finding $\min ||\hat{\mathbf{w}}||_1$, where $\hat{\mathbf{w}}$ gathers all $||\tilde{\mathbf{w}}_n||_2$ for $n = 0, \ldots, N-1$,

$$\hat{\mathbf{w}} = [||\tilde{\mathbf{w}}_0||_2, ||\tilde{\mathbf{w}}_1||_2, \ldots, ||\tilde{\mathbf{w}}_{N-1}||_2]^T. \quad (18)$$

Moreover, to impose DM constraints on all constellation points, the following matrices are constructed

$$\mathbf{W} = [\mathbf{w}_0, \mathbf{w}_1, \ldots, \mathbf{w}_{M^2-1}], \quad (19)$$

$$\mathbf{P}_{SL} = [\mathbf{p}_{SL,0}, \mathbf{p}_{SL,1}, \ldots, \mathbf{p}_{SL,M^2-1}]^T, \quad (20)$$

$$\mathbf{P}_{ML} = [\mathbf{p}_{ML,0}, \mathbf{p}_{ML,1}, \ldots, \mathbf{p}_{ML,M^2-1}]^T. \quad (21)$$

As the reweighted l_1 norm minimization has a closer approximation to the l_0 norm [37]–[39], the corresponding iteration based formulations for sparse array design becomes

$$\begin{aligned} &\min_{\mathbf{W}} \sum_{n=0}^{N-1} \delta_n^u ||\tilde{\mathbf{w}}_n^u||_2 \\ &\text{subject to } ||\mathbf{P}_{SL} - (\mathbf{W}^u)^H \mathbf{S}_{SL}||_2 \le \alpha \\ &\qquad (\mathbf{W}^u)^H \mathbf{S}_{ML} = \mathbf{P}_{ML}, \end{aligned} \quad (22)$$

where the superscript u indicates the u-th iteration, and δ_n is the reweighting term for the n-th row of coefficients, given by $\delta_n^u = (||\tilde{\mathbf{w}}_n^{u-1}||_2 + \xi)^{-1}$. The above problem can be solved using cvx, a package for specifying and solving convex problems [40], [41].

To receive and separate two orthogonally polarized signals, a crossed-dipole antenna or array is needed [30], and polarizations of the antennas at the receiver side in the desired direction do not need to match those of the transmitted signals, as cross-interference due to polarisation mismatch can be suppressed using standard signal processing techniques such as the Wiener filter when a reference signal is available [20].

IV. DESIGN EXAMPLES

In this section, design examples are provided to show the performance of the proposed design methods for both ULAs and sparse antenna arrays. For each of s_1 and s_2, the desired response is a value of one (magnitude) with a given phase at the mainlobe (QPSK), i.e., symbols '00', '01', '11', '10' correspond to 45°, 135°, −45° and −135°, respectively, and a value of 0.1 (magnitude) with random phase over the sidelobe regions. Therefore, for signals s_1 and s_2 transmitted simultaneously, we can construct 16 different combined symbols. The polarisation states for s_1 are defined by $(\gamma_1, \eta_1) = (0°, 0°)$ for a horizontal polarisation, and $(\gamma_2, \eta_2) = (90°, 0°)$ for s_2 for a vertical polarisation. Moreover, both broadside and off-broadside designs are studied. For broadside design, the mainlobe direction is assumed to be $\theta_{ML} = 0°$ for $\phi = 90°$ and the sidelobe regions are $\theta_{SL} \in [5°, 90°]$ for $\phi = \pm 90°$. For the off-broadside design, the desired direction is $\theta_{ML} = 30°$ for $\phi = 90°$, while the sidelobe regions are $\theta_{SL} \in \{[0, 25°], [35°, 90°]\}$ for $\phi = 90°$, and $\theta_{SL} \in [0, 90°]$ for $\phi = -90°$, sampled every 1°.

For sparse antenna array design, to have a fair comparison, we first obtain the DM result by (14) based on a 9λ aperture ULA with a half wavelength spacing between adjacent antennas. Then we set the error norm between the desired and designed responses from (14) as the allowed difference α in (22) for sparse array designs.

To verify the performance of each design, the corresponding beam and phase patterns are given. Moreover, bit error rate (BER) is calculated based on in which quadrant the received point lies in the complex plane. Here the signal to noise ratio (SNR) is set at 12 dB in the mainlobe direction, then with the average power (1) of all randomly generated 10^6 transmitted bits in the mainlobe, the noise variance σ^2 is 0.0631. Assuming the additive white Gaussian noise (AWGN) level is the same for all directions, then a random noise with this power level can be generated for each direction.

A. ADVANTAGE OF THE POLARISATION DESIGN OVER UN-POLARISATON'S

Fig. 2 shows the channel capacity verse SNR. Here the bandwidth of the channel is set to 1MHz, then we can see that with an increased SNR, channel capacity grow for both designs, and the channel capacity for polarisation design is two times more than non-polarization's.

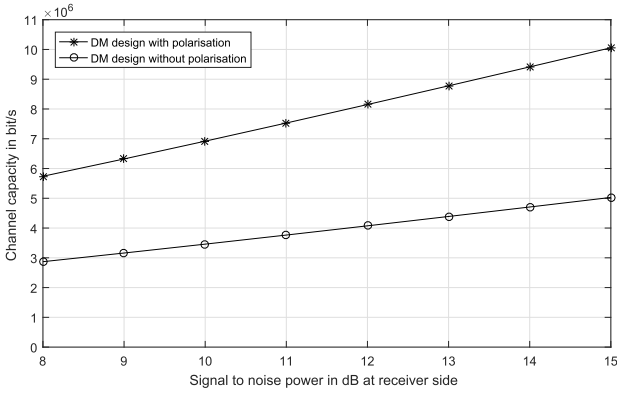

FIGURE 2. Channel capacity verse SNR at the desired location.

B. BROADSIDE EXAMPLES OF POLARISATION DESIGN

Based on the given antenna array design in (14), Fig. 3 shows the beam responses for symbols '00,00', '00,01', '00,11' and '00,10'. It can be observed that all main beams are exactly pointed to 0° (the desired direction) with a low sidelobe level. The mainlobe power level for the composite signal $s_{Re} = s_1 + s_2 j$ is 3.01dB ($\sqrt{2}$ magnitude), and its corresponding components for s_1 and s_2 coincide in the mainlobe

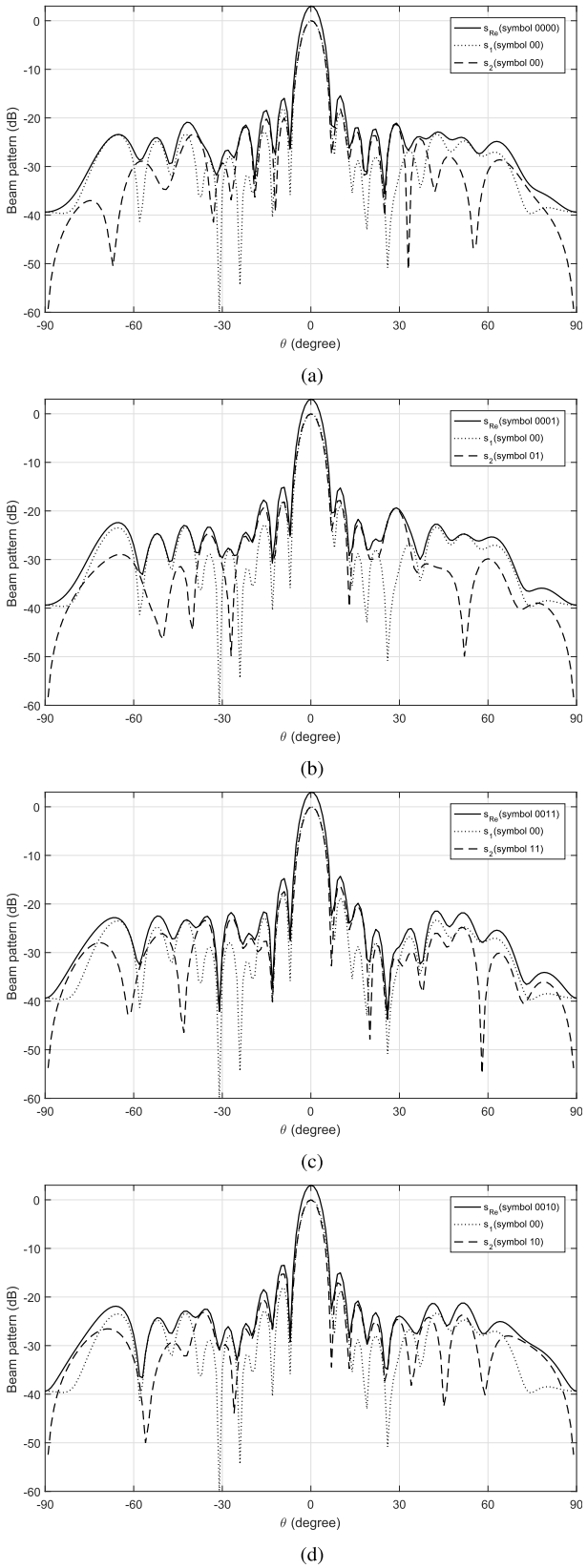

FIGURE 3. Resultant beam responses based on the broadside ULA design (14) for symbols (a) '00,00', (b)'00,01', (c)'00,11', (d)'00,10'.

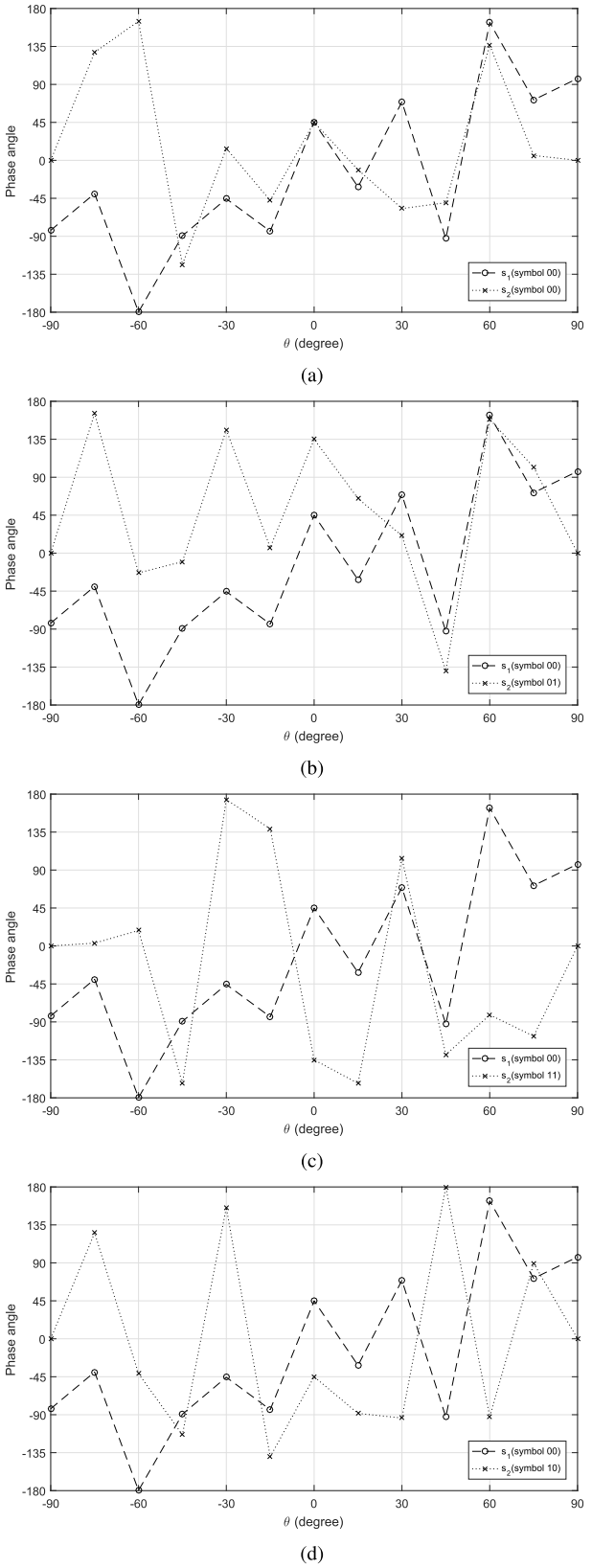

FIGURE 4. Resultant phase responses based on the broadside ULA design (14) for symbols (a) '00,00', (b) '00,01', (c) '00,11', (d) '00,10'.

direction with 0dB power level. The phases of s_1 and s_2 are shown Fig. 4, where in the desired direction the phases are in accordance with the standard QPSK constellation, while phases are random for the rest of the angles. The beam and

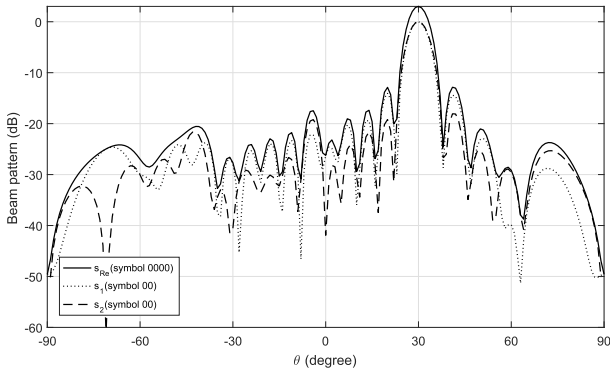

(a)

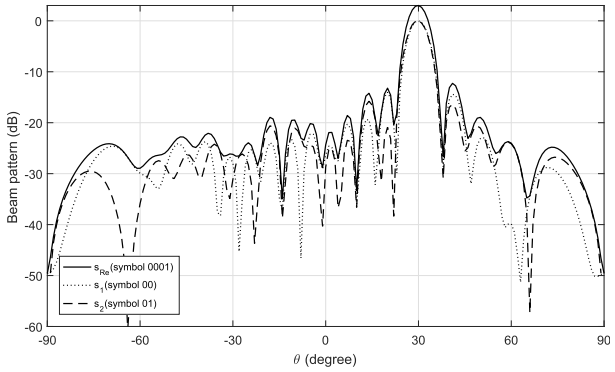

(b)

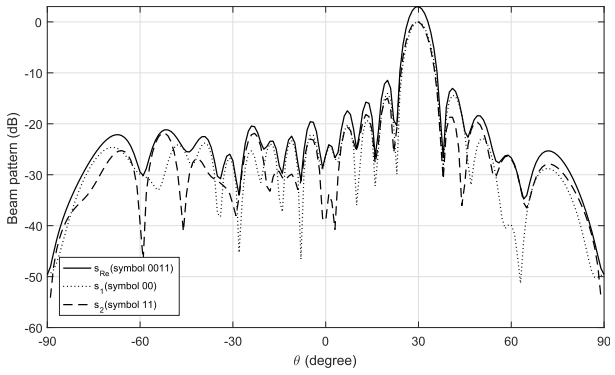

(c)

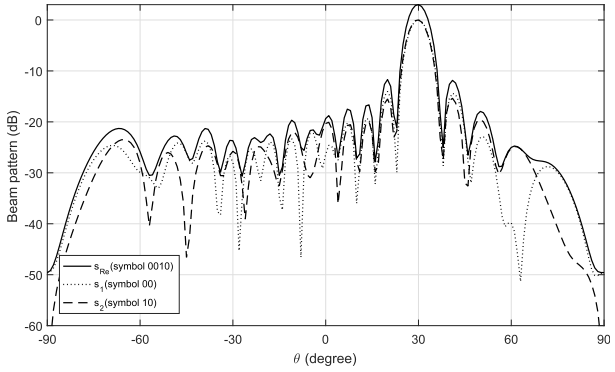

(d)

FIGURE 5. Resultant beam responses based on the off-broadside ULA design (14) for symbols (a) '00,00', (b) '00,01', (c) '00,11', (d) '00,10'.

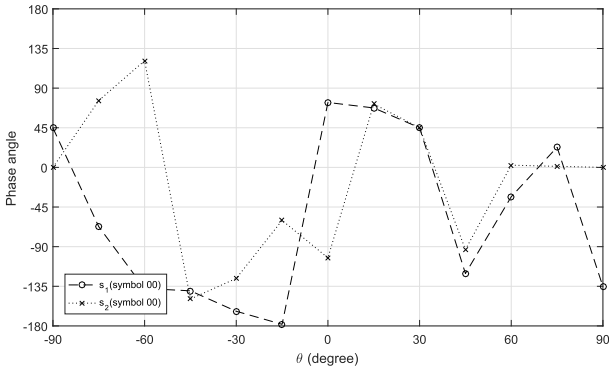

(a)

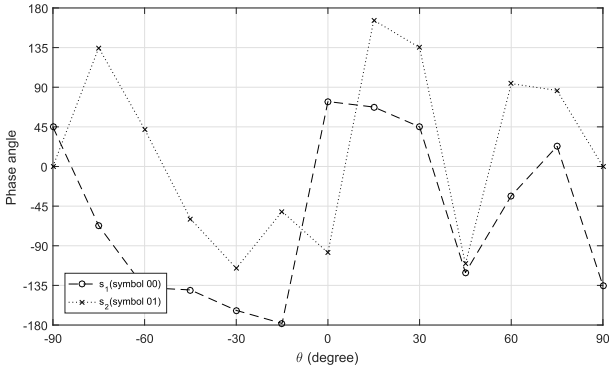

(b)

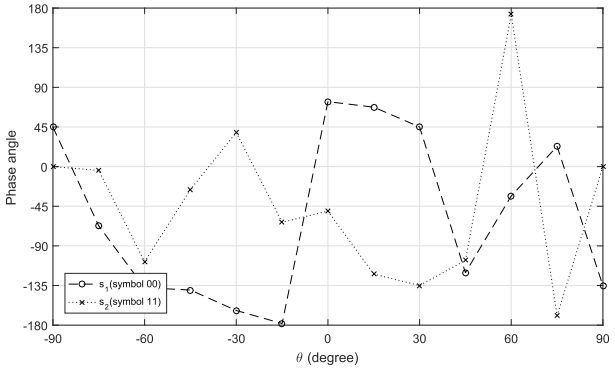

(c)

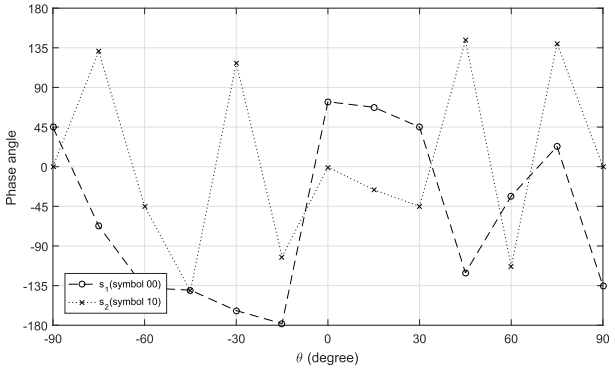

(d)

FIGURE 6. Resultant phase responses based on the off-broadside ULA design (14) for symbols (a) '00,00', (b) '00,01', (c) '00,11', (d) '00,10'.

phase patterns for other symbols are not shown as they have the same features as the aforementioned figures.

Based on the value of error norm α from the above ULA design result, the maximum aperture of the designed

crossed-dipole array is set to be 20λ with 201 equally spaced potential antennas. Moreover, $\xi = 0.001$ indicates the threshold for active antennas.

For the reweighted l_1 norm minimization method in (22), the number of active antennas is 14, with an average spacing of 0.9231λ, where the antenna locations are given in Table 1. The beam and phase patterns for these 16 combined symbols are similar to the ULA design, all indicating a satisfactory DM design result.

TABLE 1. Optimized antenna locations based on the reweighted l_1 norm minimization for off-broadside design.

n	d_n/λ	n	d_n/λ	n	d_n/λ
0	0	5	4.7	10	9.2
1	1	6	5.6	11	10.2
2	1.9	7	6.5	12	11.1
3	2.8	8	7.4	13	12
4	3.7	9	8.3		

C. OFF-BROADSIDE EXAMPLES OF POLARISATION DESIGN

Figs. 5 and 6 show the beam and phase responses for the corresponding symbols '00,00', '00,01', '00,11' and '00,10' based on the ULA design, respectively. It can be seen that all main beams are exactly pointed to 30° (the desired direction) with a low sidelobe level, and phases in this direction follow QPSK modulation pattern with scrambled values in other directions. The beam and phase patterns for other symbols have the same features as the aforementioned figures. The sparse array designs produce similar patterns to the ULA design, and the optimized locations are shown in Table 3, with the performance results in Table 4.

D. BER FOR BROADSIDE AND OFF-BROADSIDE DESIGNS

BER can be represented by the following equation

$$BER = \frac{Error\ bits}{Total\ number\ of\ bits}. \tag{23}$$

Fig. 7 shows the BER performance based on broadside and off-broadside ULA designs. Sparse array designs have a similar result. Here we can see that for both designs the achieved BER is down to 10^{-5} in desired directions, while at other directions it fluctuates around 0.5.

Note that some BER values are higher than 0.5, which is possible, because in the design, even without having any noise at the receiver side, there is already a phase bias in the received signal, resulted from scrambled phases setting for pattern synthesis, due to the DM design. For example, assume we want to send the symbol 00 using the constellation point (1, 1) in the desired direction, and the resultant constellation coordinates in another direction could be (−0.3, −0.4), which ends up representing '11', with complete error for these two bits.

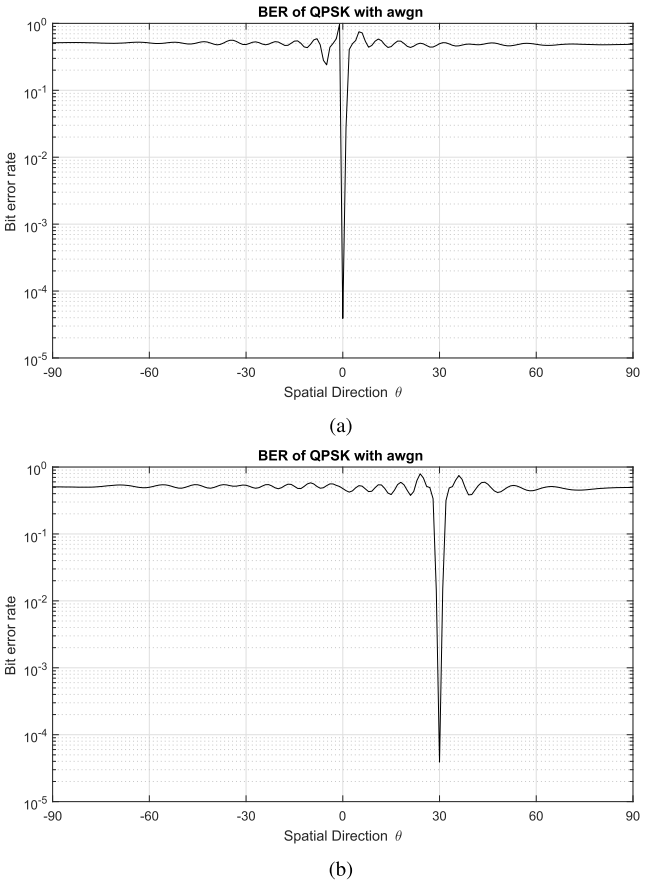

FIGURE 7. BER performance: (a) broadside ULA design, (b) off-broadside ULA design.

TABLE 2. Summary of the broadside design results.

	ULA	Reweighted l_1
Antenna number	19	14
Aperture/λ	9	12
Average spacing/λ	0.5	0.9231
$\|\|\mathbf{P}_{SL} - \mathbf{W}^H\mathbf{S}_{SL}\|\|_2$	7.9968	7.8547

TABLE 3. Optimized antenna locations based on the reweighted l_1 norm minimization for off-broadside design.

n	d_n/λ	n	d_n/λ	n	d_n/λ
0	0	6	5	12	8.4
1	1.3	7	5.8	13	9
2	1.8	8	6.3	14	9.5
3	3.2	9	6.9	15	10.3
4	3.7	10	7.5	16	10.6
5	4.6	11	7.9	17	11.3

TABLE 4. Summary of the off-broadside design results.

	ULA	Reweighted l_1
Antenna number	19	18
Aperture/λ	9	11.3
Average spacing/λ	0.5	0.6647
$\|\|\mathbf{P}_{SL} - \mathbf{W}^H\mathbf{S}_{SL}\|\|_2$	8.7887	8.7875

V. CONCLUSIONS

A crossed-dipole antenna array for directional modulation is proposed, and array designs for two signals s_1 and s_2 with orthogonal polarisation states transmitted to the same

direction at the same frequency are studied. The channel capacity based on the polarisation design doubles the capacity for the case where polarisation information is not considered, which is the main advantage resulted from the proposed scheme. The proposed design is first applied to a given antenna array geometry, and a closed-form solution is provided. Then, the proposed design is introduced to sparse arrays for finding optimized antenna locations via the reweighted l_1 norm minimization method. As shown in the provided design examples, the resultant main beams can point to the desired direction (either broadside or off-broadside) with desired phase pattern, while a low sidelobe level and scrambled phases are formed in other directions.

REFERENCES

[1] A. Babakhani, D. B. Rutledge, and A. Hajimiri, "Transmitter architectures based on near-field direct antenna modulation," *IEEE J. Solid-State Circuits*, vol. 43, no. 12, pp. 2674–2692, Dec. 2008.

[2] A. Babakhani, D. B. Rutledge, and A. Hajimiri, "Near-field direct antenna modulation," *IEEE Microw. Mag.*, vol. 10, no. 1, pp. 36–46, Feb. 2009.

[3] M. P. Daly and J. T. Bernhard, "Beamsteering in pattern reconfigurable arrays using directional modulation," *IEEE Trans. Antennas Propag.*, vol. 58, no. 7, pp. 2259–2265, Jul. 2010.

[4] M. P. Daly and J. T. Bernhard, "Directional modulation technique for phased arrays," *IEEE Trans. Antennas Propag.*, vol. 57, no. 9, pp. 2633–2640, Sep. 2009.

[5] B. Zhang, W. Liu, and X. Gou, "Compressive sensing based sparse antenna array design for directional modulation," *IET Microw., Antennas Propag.*, vol. 11, no. 5, pp. 634–641, Apr. 2017.

[6] B. Zhang and W. Liu, "Multi-carrier based phased antenna array design for directional modulation," *IET Microw., Antennas Propag.*, vol. 12, no. 5, pp. 765–772, Apr. 2018.

[7] J. Hu, S. Yan, F. Shu, J. Wang, J. Li, and Y. Zhang, "Artificial-noise-aided secure transmission with directional modulation based on random frequency diverse arrays," *IEEE Access*, vol. 5, pp. 1658–1667, 2017.

[8] F. Shu, L. Xu, J. Wang, W. Zhu, and Z. Xiaobo, "Artificial-noise-aided secure multicast precoding for directional modulation systems," *IEEE Trans. Veh. Technol.*, vol. 67, no. 7, pp. 6658–6662, Jul. 2018.

[9] F. Shu, X. Wu, J. Hu, J. Li, R. Chen, and J. Wang, "Secure and precise wireless transmission for random-subcarrier-selection-based directional modulation transmit antenna array," *IEEE J. Sel. Areas Commun.*, vol. 36, no. 4, pp. 890–904, Apr. 2018.

[10] F. Shu *et al.*, "Low-complexity and high-resolution DOA estimation for hybrid analog and digital massive MIMO receive array," *IEEE Trans. Commun.*, vol. 66, no. 6, pp. 2487–2501, Jun. 2018.

[11] T. Hong, M.-Z. Song, and Y. Liu, "Dual-beam directional modulation technique for physical-layer secure communication," *IEEE Antennas Wireless Propag. Lett.*, vol. 10, pp. 1417–1420, 2011.

[12] H. Shi and A. Tennant, "Enhancing the security of communication via directly modulated antenna arrays," *IET Microw., Antennas Propag.*, vol. 7, no. 8, pp. 606–611, Jun. 2013.

[13] Y. Ding and V. Fusco, "Directional modulation transmitter radiation pattern considerations," *IET Microw., Antennas Propag.*, vol. 7, no. 15, pp. 1201–1206, Dec. 2013.

[14] T. Xie, J. Zhu, and Y. Li, "Artificial-noise-aided zero-forcing synthesis approach for secure multi-beam directional modulation," *IEEE Commun. Lett.*, vol. 22, no. 2, pp. 276–279, Feb. 2018.

[15] W. Zhu *et al.*, "Secure precise transmission with multi-relay-aided directional modulation," in *Proc. 9th Int. Conf. Wireless Commun. Signal Process. (WCSP)*, Oct. 2017, pp. 1–5.

[16] B. Guo, Y.-H. Yang, G. Xin, and Y.-Q. Tang, "Combinatorial interference directional modulation for physical layer security transmission," in *Proc. IEEE Inf. Technol., Netw., Electron. Autom. Control Conf.*, May 2016, pp. 710–713.

[17] M. Hafez, T. Khattab, T. Elfouly, and H. Arslan, "Secure multiple-users transmission using multi-path directional modulation," in *Proc. IEEE Int. Conf. Commun. (ICC)*, May 2016, pp. 1–5.

[18] B. Zhang and W. Liu, "Antenna array based positional modulation with a two-ray multi-path model," in *Proc. IEEE 10th Sensor Array Multichannel Signal Process. Workshop (SAM)*, Sheffield, U.K., Jul. 2018, pp. 203–207.

[19] B. Zhang, W. Liu, and X. Lan, "Directional modulation design based on crossed-dipole arrays for two signals with orthogonal polarisations," in *Proc. Eur. Conf. Antennas Propag. (EuCAP)*, London, U.K., Apr. 2018.

[20] W. Liu, "Channel equalization and beamforming for quaternion-valued wireless communication systems," *J. Franklin Inst.*, vol. 354, no. 18, pp. 8721–8733, 2017.

[21] O. M. Isaeva and V. A. Sarytchev, "Quaternion presentations polarization state," in *Proc. IEEE 2nd Top. Symp. Combined Opt.-Microw. Earth Atmos. Sens.*, Atlanta, GA, USA, Apr. 1995, pp. 195–196.

[22] L. H. Zetterberg and H. Brändström, "Codes for combined phase and amplitude modulated signals in a four-dimensional space," *IEEE Trans. Commun.*, vol. 25, no. 29, pp. 943–950, Sep. 1977.

[23] R. T. Compton, Jr., "On the performance of a polarization sensitive adaptive array," *IEEE Trans. Antennas Propag.*, vol. AP-29, no. 5, pp. 718–725, Sep. 1981.

[24] R. Compton, Jr., "The tripole antenna: An adaptive array with full polarization flexibility," *IEEE Trans. Antennas Propag.*, vol. 29, no. 6, pp. 944–952, Nov. 1981.

[25] A. Nehorai and E. Paldi, "Electromagnetic vector-sensor array processing," in *Digital Signal Processing Handbook*. Boca Raton, FL, USA: CRC Press, 1998, pp. 65.1–65.26.

[26] S. Miron, N. Le Bihan, and J. I. Mars, "Quaternion-MUSIC for vector-sensor array processing," *IEEE Trans. Signal Process.*, vol. 54, no. 4, pp. 1218–1229, Apr. 2006.

[27] X. Gou, Y. Xu, Z. Liu, and X. Gong, "Quaternion-Capon beamformer using crossed-dipole arrays," in *Proc. IEEE 4th Int. Symp. Microw., Antenna, Propag. EMC Technol. Wireless Commun. (MAPE)*, Beijing, China, Nov. 2011, pp. 34–37.

[28] M. Hawes and W. Liu, "Design of fixed beamformers based on vector-sensor arrays," *Int. J. Antennas Propag.*, vol. 2015, pp. 181937.1–181937.9, Mar. 2015.

[29] J. J. Xiao and A. Nehorai, "Optimal polarized beampattern synthesis using a vector antenna array," *IEEE Trans. Signal Process.*, vol. 57, no. 2, pp. 576–587, Feb. 2009.

[30] X. Lan and W. Liu, "Fully quaternion-valued adaptive beamforming based on crossed-dipole arrays," *Electronics*, vol. 6, no. 2, p. 34, Apr. 2017.

[31] A. Moffet, "Minimum-redundancy linear arrays," *IEEE Trans. Antennas Propag.*, vol. AP-16, no. 2, pp. 172–175, Mar. 1968.

[32] H. L. Van Trees, *Optimum Array Processing: Part IV of Detection, Estimation, and Modulation Theory*. New York, NY, USA: Wiley, 2002.

[33] Q. Shen, W. Liu, W. Cui, S. Wu, Y. D. Zhang, and M. G. Amin, "Low-complexity direction-of-arrival estimation based on wideband co-prime arrays," *IEEE/ACM Trans. Audio, Speech, Language Process.*, vol. 23, no. 9, pp. 1445–1456, Sep. 2015.

[34] G. A. Deschamps, "Techniques for handling elliptically polarized waves with special reference to antennas: Part II—Geometrical representation of the polarization of a plane electromagnetic wave," *Proc. IRE*, vol. 39, no. 5, pp. 540–544, May 1951.

[35] X. Zhang, W. Liu, Y. Xu, and Z. Liu, "Quaternion-valued robust adaptive beamformer for electromagnetic vector-sensor arrays with worst-case constraint," *Signal Process.*, vol. 104, pp. 274–283, Nov. 2014.

[36] M. Hawes, W. Liu, and L. Mihaylova, "Compressive sensing based design of sparse tripole arrays," *Sensors*, vol. 15, no. 12, pp. 31056–31068, 2015.

[37] E. J. Candès, M. B. Wakin, and S. P. Boyd, "Enhancing sparsity by reweighted ℓ_1 minimization," *J. Fourier Anal. Appl.*, vol. 14, nos. 5–6, pp. 877–905, 2008.

[38] G. Prisco and M. D'Urso, "Maximally sparse arrays via sequential convex optimizations," *IEEE Antennas Wireless Propag. Lett.*, vol. 11, pp. 192–195, Feb. 2012.

[39] B. Fuchs, "Synthesis of sparse arrays with focused or shaped beampattern via sequential convex optimizations," *IEEE Trans. Antennas Propag.*, vol. 60, no. 7, pp. 3499–3503, Jul. 2012.

[40] M. Grant and S. Boyd, "Graph implementations for nonsmooth convex programs," in *Recent Advances in Learning and Control* (Lecture Notes in Control and Information Sciences), V. Blondel, S. Boyd, and H. Kimura, Eds. Berlin, Germany: Springer-Verlag, 2008, pp. 95–110. [Online]. Available: http://stanford.edu/~boyd/graph_dcp.html

[41] CVX Research. (Sep. 2012). *CVX: MATLAB Software for Disciplined Convex Programming, Version 2.0 Beta*. [Online]. Available: bhttp://cvxr.com/cvx

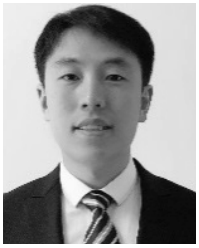

BO ZHANG received the B.Sc. degree from Tianjin Normal University, China, in 2011, and the M.Sc. and Ph.D. degrees from the Department of Electrical and Electronic Engineering, The University of Sheffield, in 2013 and 2018, respectively.

He is currently with the College of Electronic and Communication Engineering, Tianjin Normal University. His research interests include array signal processing (beamforming and direction of arrival estimation), directional modulation, and sparse array design.

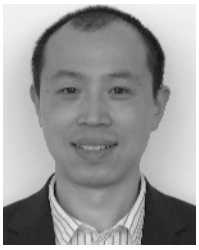

WEI LIU (S'01–M'04–SM'10) received the B.Sc. and LL.B. degrees from Peking University, China, in 1996 and 1997, respectively, the M.Phil. degree from The University of Hong Kong, in 2001, and the Ph.D. degree from the School of Electronics and Computer Science, University of Southampton, U.K., in 2003.

He held a postdoctoral position first at the University of Southampton and later at the Department of Electrical and Electronic Engineering, Imperial College London. Since 2005, he has been with the Department of Electronic and Electrical Engineering, The University of Sheffield, U.K., first as a Lecturer and then as a Senior Lecturer. He has published more than 250 journal and conference papers, three book chapters, and a research monograph about wideband beamforming *Wideband Beamforming: Concepts and Techniques* (John Wiley, 2010) and book *Low-Cost Smart Antennas* (Wiley-IEEE, 2019). His research interests include a wide range of topics in signal processing, with a focus on sensor array signal processing (beamforming and source separation/extraction, direction of arrival estimation, target tracking, and localization), and its various applications, such as robotics and autonomous vehicles, human computer interface, big data analytics, radar, sonar, satellite navigation, and wireless communications.

Dr. Liu is a member of the Digital Signal Processing Technical Committee of the IEEE Circuits and Systems Society and the Sensor Array and Multichannel Signal Processing Technical Committee of the IEEE Signal Processing Society (Vice-Chair, since 2019). He is an Associate Editor for the IEEE TRANSACTIONS ON SIGNAL PROCESSING and the IEEE ACCESS and an Editorial Board Member of *Frontiers of Information Technology and Electronic Engineering*.

XIANG LAN received the B.Sc. degree from the Huazhong University of Science and Technology, China, in 2012, and the M.Sc. degree from the Department of Electrical and Electronic Engineering, The University of Sheffield, in 2014, where he is currently pursuing the Ph.D. degree. His research interests include signal processing based on vector sensor array (beamforming and DOA estimation with polarized signals) and sparse array processing.